PHILOSOPHICAL TRANSACTIONS OF THE ROYAL SOCIETY A MATHEMATICAL, PHYSICAL & ENGINEERING SCIENCES

Surface Extended X-ray Absorption Fine Structure: Critical Appraisal of a Structural Tool for Adsorbates [and Discussion]

Geraldine Lamble, D. A. King, J. Wong and D. Norman

Phil. Trans. R. Soc. Lond. A 1986 **318**, 203-217
doi: 10.1098/rsta.1986.0072

Phil. Trans. R. Soc. Lond. A **318**, 203–217 (1986) [203]
Printed in Great Britain

Surface extended X-ray absorption fine structure: critical appraisal of a structural tool for adsorbates

By Geraldine Lamble and D. A. King
The Donnan Laboratories, University of Liverpool, Liverpool L69 3BX, U.K.

The availability of intense, tunable, polarized X-radiation from electron storage rings has led to the successful application of surface extended X-ray absorption fine structure (s.e.X.a.f.s.) measurements to the determination of inter-atomic spacings and, by using multishell analyses, complete structures for adsorbates on surfaces. Recent work on a surface iodide structure on Ni{100}, Ag{100}–$c(2\times2)$Cl, Ag{111}–$(\sqrt{3}\times\sqrt{3})$ R 30°–Cl (0.7 fractional monolayer coverage) and disordered 0.4 monolayer Ag{111}–Cl structure are reviewed. The results for Cl on Ag{100} confirm a previous exhaustive l.e.e.d. intensity analysis for the same system, but yield greater precision in the Cl–Ag bond length (2.69 ± 0.03 Å). Studies of Cl on Ag{111} were extended to low crystal temperatures, and demonstrate: (i) a significant improvement in signal quality; (ii) removal of anomalies due to anharmonicity at room temperature; and (iii) the ability of s.e.X.a.f.s., by using a multishell data analysis procedure including four atomic shells, to provide an unambiguous structure determination from both a poorly ordered and a disordered structure. The Cl–Ag bond length is found to be 2.70 ± 0.01 Å at both 0.4 and 0.7 fractional monolayer coverages.

1. Introduction

The major method currently in use for determining surface structures is low-energy electron diffraction (l.e.e.d.) intensity analysis. It was proposed by Lee (1976) that the bulk technique of extended X-ray absorption fine structure (e.X.a.f.s.) could be applied to surfaces for the determination of bond distances and adsorption sites for adsorbates. The first successful experiments were reported by Citrin *et al.* (1978). Although the technique is inherently experimentally more demanding than l.e.e.d., surface e.X.a.f.s. is dominated by single scattering; single-electron, short-range order theories suffice to extract accurate data. L.e.e.d. analysis, on the other hand, requires the application of a full multiple scattering theory. As shown by Marsh & King (1979), attempts to apply Fourier transform techniques to l.e.e.d. intensity spectra proved fruitless, whereas these techniques have proved highly successful in e.X.a.f.s. data analysis. Data analysis in s.e.X.a.f.s. is therefore more direct, less ambiguous, and less tedious than in l.e.e.d., providing a major incentive for persevering with the experimental difficulties involved.

In e.X.a.f.s., monochromatic-light radiation is energy scanned across an atomic band edge, and the light absorption, due to photoemission from the appropriate core level, is measured as a function of photon energy. Above the band edge, fine structure is observed in the absorption. Disregarding the near-edge structure (in the region up to *ca.* 50 eV above the edge), this structure arises from changes in the final state wavefunction as a result of interference between the outgoing photoelectron wave from an absorber atom with the backscattering electron waves from neighbouring atoms. The interference may be constructive or destructive,

depending on the wavelength of the photoelectron wave with respect to the distance between the absorbing and backscattering atom and their phaseshifts. E.X.a.f.s. is therefore a local effect depending on inter-atomic distances, because the transition matrix element is finite only over the atomic spatial region. Only the local character of the final state wavefunction affects the core matrix elements. As the photon energy is increased, so the final state modulates together with the absorption probability, and hence also with the absorption coefficient μ, where $\mu x = \ln (I_0/I)$; I_0 is the incident light intensity, I is the transmitted intensity, and x is the thickness of the absorbing sample.

In principle, any process that is proportional to the rate of absorption of radiation can be used to measure e.X.a.f.s. The creation of a core hole will give rise to Auger electron emission and to fluorescence. Surface sensitivity in e.X.a.f.s. can be achieved by monitoring the adsorbate edge to achieve maximum surface sensitivity, and by measuring (i) the elastic Auger channel, (ii) the fluorescence yield, (iii) the total secondary electron yield, or (iv) a partial secondary electron yield. The secondaries consist mainly of inelastic Auger electrons and the cascade resulting from Auger emission. Since the elastic Auger energy remains the same with increasing photon energy above the edge, all the channels of the resulting cascade will be the same, and the resulting yield modulates with the rate of core hole creation. In their pioneering work Citrin *et al.* (1978) used the elastic Auger channel, while the secondary-electron yield technique was developed by Stöhr *et al.* (1978). An ion yield detection technique, based on photon-stimulated desorption, has been used by Jaeger *et al.* (1980). The direct detection of the photoelectrons emitted from the core hole will, however, not be a good measure of e.X.a.f.s., since the direct photoelectron has a continuously changing energy, and the detected yield will be both energy and angle dependent. Electrons excited by the photoelectron also have continuously changing scattering channels. However, except for atoms of low atomic number, the major elastic Auger channel is at a far higher energy than that of the direct photoelectron, so that the total secondary-electron yield is dominated by this process.

2. Experimental

Measurements of surface e.X.a.f.s. spectra were made on station 3, beamline 6 of the synchrotron radiation source (s.r.s.) at the S.E.R.C. Daresbury Laboratory. A schematic diagram of the experimental station is shown in figure 1. A double-focusing toroidal gold-coated pre-mirror focuses 4 mrad of horizontal radiation from the storage ring through a double-crystal constant-deviation monochromator onto the sample. The high-energy cut-off dictated by this pre-mirror is about 12 keV. A range of carbon, beryllium and aluminium filters with varying attenuation characteristics are situated in front of the pre-mirror. The filters act as a low-energy cut-off eliminating the u.v. and visible component of the synchrotron radiation, which would otherwise be transmitted by the double-crystal monochromator by normal reflections. Everything between the storage ring and the sample chamber is in ultra-high vacuum. All operations of the optical elements in the monochromator are controlled externally by computer-operated stepping motors via a CAMAC hardware system. Details of the s.e.X.a.f.s. monochromator are reported by MacDowell *et al.* (1985).

The pre-mirror demagnifies the s.r.s. by a factor of 2:1 at the sample. The spot size at the sample is typically 1 mm (vertical) by 3 mm (horizontal (f.w.h.m.)). Since heating effects in the monochromator caused vertical beam movements at the sample, a large sample size was

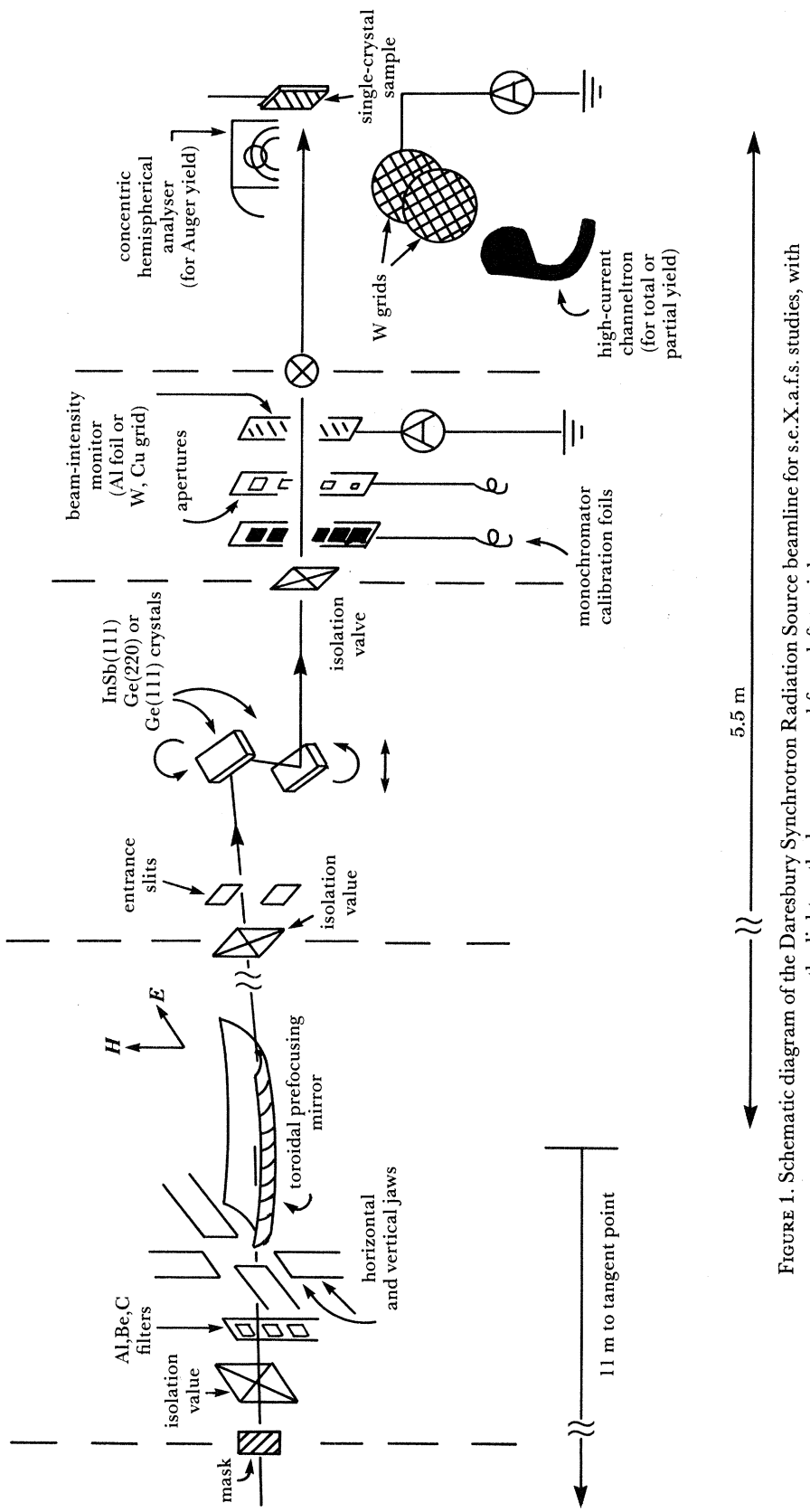

FIGURE 1. Schematic diagram of the Daresbury Synchrotron Radiation Source beamline for s.e.X.a.f.s. studies, with the light path shown arrowed from left to right.

required to ensure that the exit beam did not track off the crystal. A set of apertures could be interposed in the beam monitor section to reduce the size of the exit beam.

The experiments were made in a conventional Vacuum Generators u.h.v. chamber with facilities for surface characterization by l.e.e.d. and Auger electron spectroscopy.

The s.e.X.a.f.s. data presented here were obtained by monitoring the total secondary-electron yield obtained via drain-current measurements from a tungsten mesh, placed about 3 cm from the crystal. This yield was referenced to the incident intensity by measuring the drain current from aluminium foil 0.75 μm thick, placed in the section between the monochromator and the sample chamber. This foil was cleaned by argon-ion bombardment, to ensure a linear response with photon energy.

Cleaning procedures for the Ni{100} sample and its 'surface iodide' are described by Jones *et al.* (1983). The silver crystals were cleaned by continuous argon-ion bombardment (10 μA, 1.5 kV) and anneal cycles at 800–870 K until no visible chlorine or sulphur peaks appeared in the Auger spectra.

An electrolytic chlorine source, consisting of a silver gauze anode and a platinum foil cathode with an 'electrolyte' composition of 1% $CdCl_2$ and 99% AgCl (by mass), was used to dose the silver crystals. Ion mobility was encouraged by heating the electrolyte pellet with a tungsten filament to 320–370 K. The chlorine surface coverage was monitored by a retarding field analyser Auger system.

To obtain data at low temperatures, the samples were mounted on a 'cold-probe' manipulator on which the sample could be heated radiatively, the temperature measurements being made with a chromel/alumel thermocouple.

Bulk e.X.a.f.s. data were obtained by doping suitable compounds with 10% (by mass) graphite to prevent charging effects, and pressing into pellets. For the low-temperature bulk studies these pellets were mounted on a copper block to increase thermal conductivity, which was then suspended from the cold probe. The secondary-electron yield technique was again used to monitor absorption.

3. The e.X.a.f.s. formalism and extraction of crystal parameters

(a) *The e.X.a.f.s. equation*

The normalized oscillatory part of the X-ray absorption coefficient can be written as

$$\chi(k) = (\mu - \mu_0)/(\mu_0 - \mu_*),$$

where μ is the total absorption, μ_0 is the monotonic atom-like absorption, or the absorption without interference effects, μ_* is the background absorption from the atoms not of interest. The background subtraction procedure is described in §3*b*.

This in turn can be written as a sum of sinusoidal waves, namely

$$\chi(k) = \sum_i S_a(k) \frac{|F_i(k)|}{k} \int \exp(-2r_i/\lambda) \sin\{2kr_i + \phi_i(k)\} \frac{P(r_i)}{r_i^2} \, \mathrm{d}r_i. \qquad (1)$$

The sum is taken over the atoms at a distance r_i from the X-ray absorbing atom; k is the photoelectron wavevector; $\phi_i(k)$ is the total phase-shift experienced by the photoelectron, which can be written as the sum of twice that due to the coulombic interaction at the absorber, $\phi_a(k)$, (since this is experienced on both outward and return journeys) and that due to the

backscattering neighbour, $\phi_b(k)$. $F_i(k)$ is the k-dependent backscattering amplitude of the neighbouring atoms. It is dependent on atomic number, Z, and is the only function in the total amplitude which has resonant behaviour in k, given by

$$F_i(k,\pi) = F_i(k)\,e^{i\phi_b(k)}.$$

Losses due to multiple excitations at the absorber due to excess energy in the photoionization process are approximated by $S_a(k)$. This is the only term in the e.X.a.f.s. amplitude that is mainly due to the absorber and is described in detail by Stern *et al.* (1980). The inelastic mean free path of the photoelectron, λ, very roughly accounts for losses to the e.X.a.f.s. amplitude caused by the finite lifetime of the photoelectron. The distribution of atoms around the absorber is denoted by $P(r_i)$, i.e. the probability that the ith backscattering atom is at r_i. It is usually assumed that this distribution is Gaussian, so that

$$P(r_i) = [(1/2\pi)^{\frac{1}{2}}\sigma_i]\,\exp[-(r-R_i^2/2\sigma_i^2)],$$

where σ_i^2 is the mean square degree of displacement, which has two components: that due to thermal lattice vibrations and that due to static disorder. The solid is then treated in the harmonic potential approximation, the formalism reducing to the generally accepted form:

$$\chi(k) = \sum_i \frac{N_i\,|F_i(k)}{kR_i^2}\exp(R_i/\lambda)\exp(-2k^2\sigma_i^2)\sin\{2kR_i+\phi_i(k)\}, \qquad (2)$$

where N_i is the number of neighbours in a shell at a distance R_i from the absorber.

As pointed out by Eisenberger & Brown (1979), anharmonic effects can be important for some systems. As discussed later (§5), for systems where anharmonicity is important the application of (2) can lead to systematic errors in bond lengths.

(*b*) *Data analytical methods*

(i) *Background subtraction*

Background subtraction is achieved by firstly choosing a reference point, usually taken to be halfway up the absorption edge. It is this marker that is used, in the curve fitting method, when lining up theoretical and experimental spectra in the determination of the photoelectron 'energy zero'. The true 'energy zero' is not known, but differences in 'energy zeros' of compounds are a measure of differences in inner potentials.

The smooth background may be subtracted in a number of ways, the most common being to define a polynomial, μ_*, to describe the absorption not of interest (for example, from the sample support or the substrate atoms) and a post-edge polynomial to describe the atomic-like absorption. Alternatively the edge jump may be simply subtracted away and a smooth polynomial drawn through the remaining data. Any background subtraction method is suitable provided that an evenly oscillating signal can be obtained in the end which contains no artifacts introduced by the method to obtain it.

(ii) *Extraction of crystal parameters*

E.X.a.f.s. analysis requires a detailed knowledge of the amplitude and phase functions for the determination of inter-atomic distances, Debye–Waller factors, and coordination numbers. Phase-shift and amplitude transferabilities from the standard to the experimental system are usually assumed, although the validity of the former can be checked empirically (Citrin *et al.* 1976; Lamble *et al.* 1985).

PHILOSOPHICAL TRANSACTIONS OF THE ROYAL SOCIETY A MATHEMATICAL, PHYSICAL & ENGINEERING SCIENCES

There have been two ways of approaching the analysis: the first, (universally used in s.e.X.a.f.s. analyses to date) being the Fourier transform method, while the second is a curve-fitting technique. The former involves an empirical derivation of phase shifts; shell contributions are separated to extract phase and amplitude functions for each shell. This neglects experimental errors and unsuitability of standard compounds. The latter depends on the phase-shift calculation used and the approximations made therein.

Our approach was effectively a combination of the two methods: (*a*) initial theoretical calculation of phase shifts; (*b*) empirical phase-shift refinement by using standard compounds; and (*c*) comparative cross-checking of resulting phase shifts by interchanging between standard compounds. This permits detection of systematic errors, for example those arising from anharmonic effects or in the phase-shift calculation. We are also able to determine a true confidence interval in inter-atomic spacings determined for compounds with known spacings by transferring phase shifts between bulk compounds. Bulk-surface phase-shift transferability was, however, assumed.

The computer program used to analyse the data is based on the original theory of Lee & Pendry (1975). It was written by Gurman *et al.* (1984) and is a rapid version of the curved-wave treatment in the original Daresbury e.X.a.f.s. program of Lee & Pendry (1975). An iterative least-squares fitting method is used on the calculated energy spectrum. The initial inputs to the program are the crystallographic data and phase shifts calculated by using the Daresbury MUFFPOT program. The latter are refined within the analysis program by using standard compounds to compensate for the inadequacies of the muffin-tin approximation for certain types of compound.

4. Surface-structure determination: room-temperature data

(*a*) *Iodine on* Ni{100}

The first system to be studied by s.e.X.a.f.s. by using the synchrotron radiation source at the S.E.R.C. Daresbury laboratory was iodine on Ni{100}. Reasons for choosing this particular system were that an extensive l.e.e.d.-with-A.e.s. study of several phases had already been made by Jones *et al.* (1983); the system is particularly stable for considerable periods of time; analogous systems (I–Ag{111} (Citrin *et al.* 1978), and Cu{100} and Cu{111} (Citrin *et al.* 1981)) had already been studied at Stanford by using the same technique; and iodine, being a reasonably heavy atom, would be expected to exhibit a large backscattering magnitude to high k, thus providing a potentially simple system to study initially.

On exposure of iodine to Ni{100} while cooling from above 620 K to room temperature, a phase forms that has been identified as a single layer of NiI_2, which is normally incommensurate with the substrate but is slightly distorted from the structure of the bulk compound and adopts preferred orientations on the surface (Jones *et al.* 1983).

This surface phase was analysed by using both a single-shell analysis with the Fourier transform technique and single-shell and multishell analyses with the curve-fitting technique (Jones *et al.* 1985). NiI_2 was used as a bulk standard to determine the required phase shifts. Data were obtained at room temperature. A comparison between the experimental, background-subtracted spectra and a calculated spectrum based on a five-shell parameter input, by using the bulk nickel-iodide structure, is shown in figure 2, with the first nearest-neighbour Ni–I bond

distance decreased by 0.05 Å† relative to that in bulk NiI_2. A similar contraction was obtained by using the Fourier transform technique. Fourier transforms of the experimental and calculated spectra of figure 2 are shown in figure 3. The 'surface iodide' structure is depicted in figure 4.

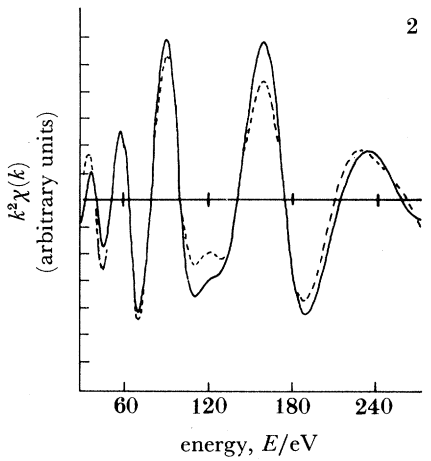

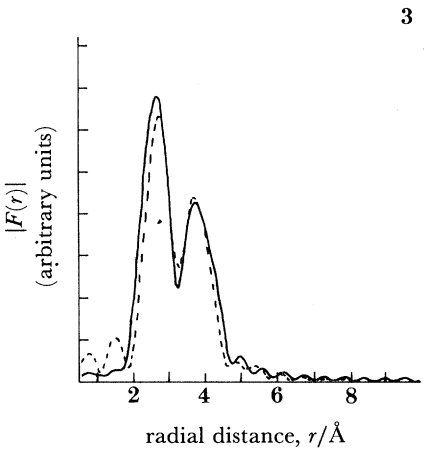

FIGURE 2. Back-transformed s.e.X.a.f.s. data of a surface iodide structure observed at an iodine coverage of two monolayers on Ni{100}, where real space components above 5 Å have been filtered out. The theoretical spectrum, represented as a broken line, is compared with the experimental spectrum, represented as a continuous line, to obtain the best least-squares fit.

FIGURE 3. Theoretical (broken line) and experimental (continuous line) radial distribution functions of the s.e.X.a.f.s. spectra, shown in figure 2, of a surface iodide structure observed after the adsorption of two monolayers of iodine on Ni{100}.

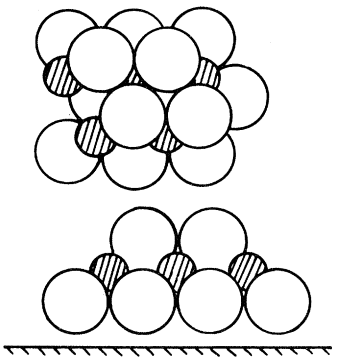

FIGURE 4. Plan and cross-sectional view of the surface iodide phase formed at a two-monolayer coverage of iodine on Ni{100}, as deduced from l.e.e.d. and s.e.X.a.f.s. analyses. The nearest-neighbour nickel–iodine distance in the surface iodide shows a contraction of 0.05 Å relative to bulk nickel iodide.

(*c*) *Chlorine adsorption on* Ag{100}: *s.e.X.a.f.s. to support l.e.e.d.*

Chlorine on Ag{100} was considered an important test system for s.e.X.a.f.s., since an exhaustive l.e.e.d. structural analysis had been made on the $c(2\times2)$ structure formed when Ag{100} is exposed to chlorine by Zanazzi *et al.* (1976). They examined a variety of models, and concluded that a simple overlayer model (s.o.m.) with Cl atoms in fourfold hollow sites

† 1 Å = 10^{-10} m = 0.1 nm.

gave best agreement between theory and experiment. The refinement of this structure with respect to non-structural parameters revealed an unusual interference between the choice of potential (and hence phase-shift) for the chlorine and the value of the distance d_z^s between the overlayer plane and first substrate layer plane, and led to the conclusion that $1.57 < d_z^s < 1.78$ Å, with a 'best value of 1.73 Å. This is equivalent to a Ag–Cl bond length R in the range $2.57 < R < 2.70$ Å, with a 'best' value of 2.67 Å. Subsequently, Greenside & Hamman (1981) calculated the electronic structure for $c(2\times2)$ Cl on Ag{100}, by using both the s.o.m. and a mixed-layer model (m.l.m.) with an epitaxial layer of AgCl on the surface, and concluded from a comparison with the photoemission spectra of Weeks & Rowe (1978) for this system that best agreement was obtained with the m.l.m. This calculation was, however, based on the bulk AgCl bond length of 2.77 Å, which is outside the limits determined by Zanazzi *et al.* (1976), and could not be regarded as seriously questioning the l.e.e.d. analysis. More recently, Citrin *et al.* (1982) made a s.e.X.a.f.s. study of a $c(2\times2)$ Cl structure on Cu{100}, which, together with further electronic structure calculations, led them to claim that they could 'resolve previously reported discrepancies for the Ag{100}–$c(2\times2)$Cl system'. They find, for Cl on Cu{100}, good agreement with a s.o.m. in both s.e.X.a.f.s. and photoemission; more pertinently to the present work, they derive a bonding radius for 'surface Cl' from Cl/Cu{100} of 1.09 Å, which, when applied to Ag{100}, gives a Cl–Ag bond length of 2.53 Å. This would move the Cl atom plane 0.38 Å closer to the Ag surface than reported by Zanazzi *et al.*, and this geometry then gives good agreement between calculated photoemission data and experiment. Citrin *et al.* (1982), unable to obtain good data for Cl on Ag{100}, comment on the desirability of obtaining an accurate value for the Cl–Ag bond length by using s.e.X.a.f.s. in the total-yield mode, which is what we have achieved.

S.e.X.a.f.s. data were collected from the Cl K-edge at 2870 eV for Ag{100}–$c(2\times2)$Cl, with the crystal at room temperature (Lamble *et al.* 1985). The data are shown in figure 5 after background subtraction, Fourier transformation, and back-transformation with a window

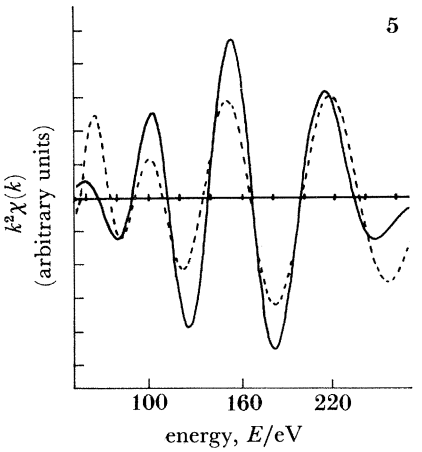

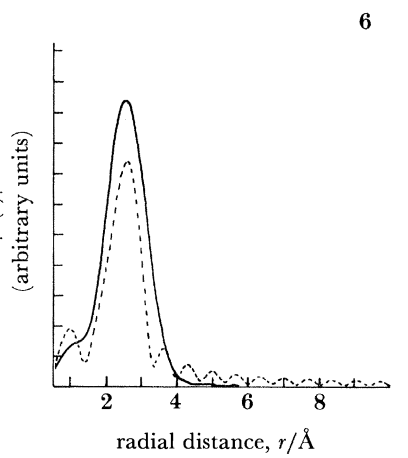

FIGURE 5. Back-transformed experimental s.e.X.a.f.s. data, represented as a continuous line, is shown together with the theoretical best least-squares fit, represented as a broken line, for the $c(2\times2)$ phase observed at saturation coverage of chlorine adsorbed on Ag{100}, where all Fourier components, other than those of the first shell, have been filtered out.

FIGURE 6. Theoretical (broken line) and experimental (continuous line) radial distribution functions for the first-shell s.e.X.a.f.s. spectra shown in figure 6 for the $c(2\times2)$ phase observed at saturation coverage of chlorine adsorbed on Ag{100}.

function eliminating all but first-shell contributions, and compared with a theoretical calculation obtained with a first shell of Ag backscattering atoms. The Fourier transforms are shown in figure 6. Best agreement is obtained with a Cl–Ag bond length of 2.69 ± 0.03 Å, and the structure is depicted in figure 7. This is in very satisfactory agreement with the 'best' value from the l.e.e.d. analysis of Zanazzi *et al.* (1976) of 2.67 Å, and confirms that there is a

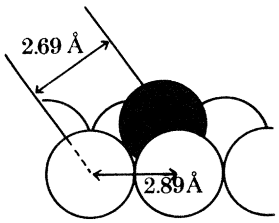

FIGURE 7. The simple overlayer model: fourfold hollow site occupation deduced by s.e.X.a.f.s. for the $c(2 \times 2)$ phase of chlorine adsorbed on Ag{100}.

significantly shorter bond length in the surface phase than in bulk AgCl (2.77 Å). The bond length is, however, significantly longer than predicted by Citrin *et al.* (1982). In our work, phase shifts were obtained by a combination of muffin-tin-based calculation and subsequent refinement by using e.X.a.f.s. data from bulk AgCl at 300 K and the known structure of AgCl. As discussed in the following section, the use of a harmonic potential approximation is subject to errors under these conditions, and the confidence interval quoted (± 0.03 Å) does take this into account. We note that there is, nevertheless, a significant improvement on the error margin quoted in the l.e.e.d. study ($+0.05$ Å with -0.13 Å).

5. Chlorine adsorbed on Ag{111}: the need for low-temperature data

Several factors led us to question the application of the harmonic potential approximation to the Cl/Ag system at 300 K. In calculating e.X.a.f.s. spectra to fit data obtained from bulk AgCl at 300 K, we concluded that surprisingly large corrections had to be made to phase shifts calculated *a priori* to reproduce the known lattice constant. Furthermore, the root mean square displacement amplitude in bulk AgCl at room temperature is 0.155 Å, which suggests that anharmonic effects could be appreciable when accuracies in the region of 0.01 Å are sought. We therefore obtained e.X.a.f.s. spectra from bulk AgCl at 300 K and at 100 K to investigate anharmonic effects. In the harmonic potential approximation, (2) is obtained for $\chi(k)$, in which the only temperature-dependent term is a Debye–Waller damping term, $\exp[-2k^2\sigma_i^2]$. Its effect is thus a simple symmetric broadening of e.X.a.f.s. amplitudes with increasing temperature. We observed, in addition to this broadening, a considerable shift in the e.X.a.f.s. frequency, leading to an apparent contraction of bond distance with increase in temperature. Between 100 and 300 K, this amounted to a 'decrease' in the Ag–Cl bond length of 0.06 Å.

Returning to (1), and following Eisenberger & Brown (1979), instead of a Gaussian pair distribution function for $P(r_i)$, anharmonicity requires an asymmetric function that yields the expression

$$\chi(k) = \sum_i \frac{N_i |F_i(k)|}{k} \{S_i^2(k) + A_i^2(k)\}^{\frac{1}{2}} \sin\{2kR_i + \phi_i(k) + \Sigma_i(k)\}, \quad (3)$$

PHILOSOPHICAL TRANSACTIONS OF THE ROYAL SOCIETY A MATHEMATICAL, PHYSICAL & ENGINEERING SCIENCES

where the anharmonicity term $\Sigma_i(k) = \arctan A_i(k)/S_i(k)$. Most importantly, there is now an additional phase term $\Sigma_i(k)$. Omitting this can lead to an apparent lattice contraction with increasing temperature, since the magnitude of $\Sigma_i(k)$ increases with temperature.

We conclude that there are two major benefits from obtaining s.e.X.a.f.s. data at low temperatures. Owing to reduction of contributions from the Debye–Waller term, signal–noise is improved; and, owing to a tendency of the term $\Sigma_i(k)$ to fall to zero at low temperatures, the harmonic potential approximation can be used to analyse the data with greater confidence. We therefore obtained data for Cl on Ag{111}, at two coverages, at 100 K (Lamble *et al.* 1985).

Bowker & Waugh (1983) have made a detailed l.e.e.d., A.e.s. and thermal desorption study of chlorine on Ag{111}, and, among other observations, confirm the formation of a weak, diffuse $(\sqrt{3}\times\sqrt{3})$ R 30° structure, which had been previously observed, and assign to it a fractional monolayer coverage of 0.7 (ratioed to the number of Ag atoms in the surface plane). A mixed-layer model was favoured for this structure; an epitaxial layer of AgCl{111} had been previously suggested by Rovida & Pratesi (1975). No l.e.e.d. patterns were observed at lower coverages, apart from the (1×1) symmetry of the substrate.

These l.e.e.d. pattern observations of Bowker & Waugh (1983) were confirmed in our study, the $(\sqrt{3}\times\sqrt{3})$ R 30° beams being broad, weak and diffuse at 0.7 monolayers of chlorine. High-quality s.e.X.a.f.s. data were collected for this structure from the Cl K-edge, with the crystal at 100 K. The data are shown in figure 8 after background-subtraction, Fourier transformation and back-transformation with a window function that includes all shells out to 5 Å. Fourier transforms are shown in figure 9. A comparison is shown with the theoretical calculation that gives the best fit to the data; this is a full multishell calculation, based on the simple overlayer model shown in figures 10 and 11. This honeycomb structure, which satisfies the l.e.e.d. symmetry, is the only trial structure that provided even a reasonable fit to the data, and variation of the intershell spacings gave the excellent fit shown with the spacings given

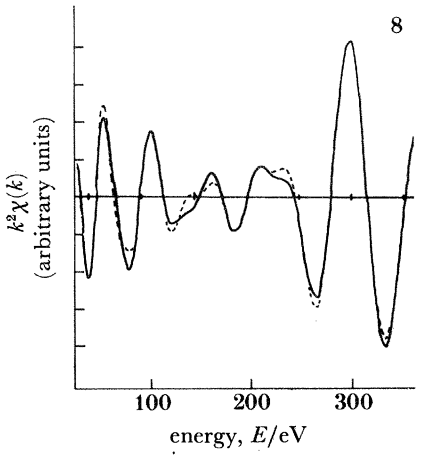

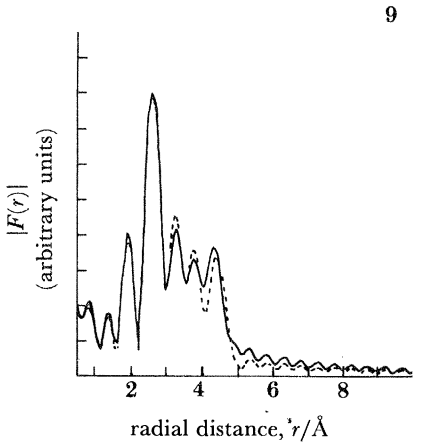

FIGURE 8. Back-transformed experimental s.e.X.a.f.s. spectrum, represented as a continuous line, is shown with the best theoretical fit, represented as the broken line for the $(\sqrt{3}\times\sqrt{3})$ R 30° phase observed when 0.7 monolayers of chlorine are adsorbed on the Ag{111} surface. Real space components above 5.2 Å have been filtered out of the data. This multishell comparison leads to the threefold hollow site 'vacancy' or 'honeycomb' model shown in figures 10 and 11.

FIGURE 9. Radial distribution functions of the experimental and theoretical s.e.X.a.f.s. spectra shown in figure 8 for 0.7 monolayers of chlorine adsorbed on Ag{111}. The theoretical transform is shown as a broken line while the experimental transform is represented as a continuous line.

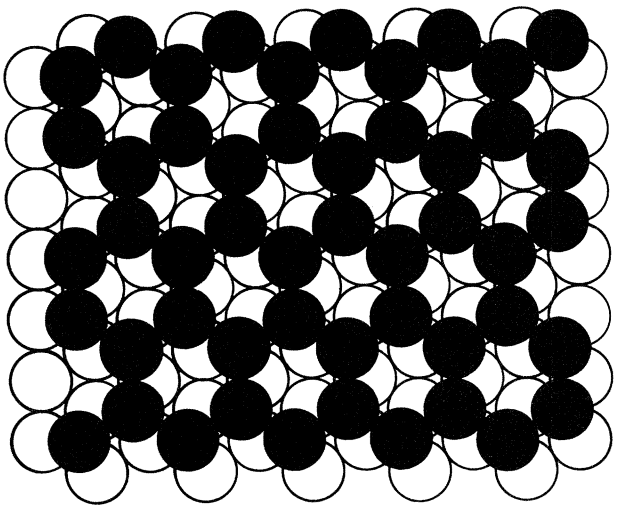

FIGURE 10. Plan view of the $(\sqrt{3} \times \sqrt{3})$ R 30° 'vacancy' or 'honeycomb' model, as deduced by s.e.X.a.f.s. for 0.7 monolayers of chlorine adsorbed on Ag{111}.

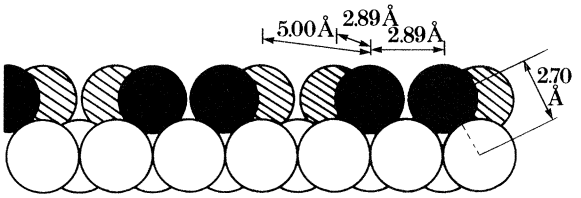

FIGURE 11. Cross-sectional view of the structure deduced by s.e.X.a.f.s. for the $(\sqrt{3} \times \sqrt{3})$ R 30° structure observed on Ag{111}, viewed along the ⟨110⟩ azimuth, after the adsorption of 0.7 monolayers of chlorine. The plan view is shown in figure 10, while the experimental and theoretical s.e.X.a.f.s. spectra and resulting Fourier transforms are shown in figure 8 and 9, respectively.

TABLE 1. A COMPARISON OF EXPERIMENTAL AND THEORETICAL REAL-SPACE COMPONENTS IN THE $(\sqrt{3} \times \sqrt{3})$ R 30° STRUCTURE OBSERVED WHEN 0.7 MONOLAYERS OF CHLORINE ARE ADSORBED ON Ag{111}

shell	number of neighbours, N_i	model bond distance, R_i/Å	experimental bond distance, R_i/Å
1. Cl–Ag	3	2.70	2.70
2. Cl–Cl	3	2.89	2.93
3. Cl–Ag	3	3.94	3.71
4. Cl–Cl	6	5.00	4.83

in table 1. The number of atoms in each shell was also varied and found to give a best fit with the structure in figure 9; however, the interplay between the Debye factor and coordination number in finding a best fit to the peak amplitudes is strong, and no great significance can be attached to these variables. The structure in figures 10 and 11 represents the first full multishell structure-determination for a submonolayer surface structure by s.e.X.a.f.s. It is worth noting that the diffuse l.e.e.d. pattern from this structure means that l.e.e.d. intensity analysis is not a viable structural technique in this instance.

A multishell s.e.X.a.f.s. analysis was also made for 0.4 monolayers of chlorine on Ag{111}, the coverage being determined from a comparison of the ratios of Cl to Ag peak heights from

A.e.s. for this structure with the 0.7 monolayer structure. Diffuse scattering superimposed on the (1×1) l.e.e.d. pattern indicated disorder in the overlayer with no tendency to form a superstructure. The data are presented in figures 12 and 13, and shell spacings are collected in table 2, corresponding to the best-fit theoretically computed s.e.X.a.f.s. spectrum. The most striking feature in comparing the analyses of the 0.4 monolayer structure with the 0.7 monolayer structure is *the absence of the first chlorine shell* at 2.9 Å in the former. The remaining shells are not only present, but are located at the same spacing for the two coverages. We conclude that the low coverage structure is a simple overlayer structure, with chlorine atoms again in the threefold hollow sites, but with avoidance of the nearest-neighbour sites depicted as filled in figure 10.

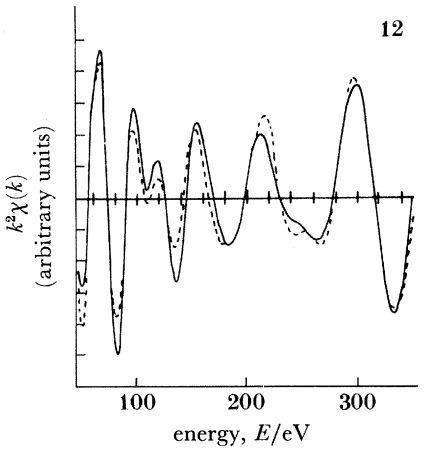

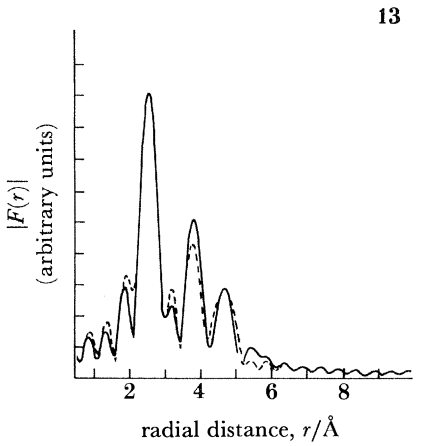

FIGURE 12. Experimental s.e.X.a.f.s. data, represented as a continuous line, is compared with the theoretical spectrum, represented as a broken line, to obtain the best least squares fit for the adsorption of 0.4 monolayers of chlorine adsorbed on Ag{111}.

FIGURE 13. Radial distribution functions of the experimental and theoretical s.e.X.a.f.s. spectra shown in figure 12 for 0.4 monolayers of chlorine adsorbed on Ag{111}. The theoretical transform is represented with a broken line, while the experimental transform is represented with a continuous line. This s.e.X.a.f.s. analysis leads to the same Ag–Cl nearest-neighbour distance as for the higher coverage structure depicted in figures 8–12.

TABLE 2. A COMPARISON OF EXPERIMENTAL AND THEORETICAL REAL-SPACE COMPONENTS IN THE PHASE FORMED WHEN 0.4 MONOLAYERS OF CHLORINE ARE ADSORBED ON Ag{111}

(The close-packed Cl–Cl component observed in the 0.7 monolayer structure is absent in this lower coverage phase, but the first nearest-neighbour Cl–Ag distance is the same for both high and low coverages.)

shell	number of neighbours, N_i	model bond distance, R_i/Å	experimental bond distance, R_i/Å
1. Cl–Ag	3	2.70	2.70
2. Cl–Ag	3	3.93	3.68
3. Cl–Cl	6	4.99	5.14

The two analyses above show a further striking feature. The Cl–Ag nearest-neighbour distance is obtained as 2.70 Å in both cases, showing a remarkable lack of dependence of bond length on coverage. It might have been anticipated that the proximity of three neighbouring Cl atoms in the 0.7 monolayer structure would provide a sufficiently repulsive interaction to cause a noticeable increase in bond length. A comparison between different sets of experimental data showed a reproducibility in the first-shell spacing of less than 0.01 Å. This is the first time that

bond lengths have been measured for a simple overlayer system at different coverages with anything approaching this accuracy.

The accuracy of the first-shell bond distance (rather than the reproducibility) depends critically on the accuracy of the phase shifts used. In our work on the Cl/Ag systems described, phase shifts were obtained by refining calculations against e.X.a.f.s. data obtained for bulk AgCl (Cl K-edge and Ag L_I edge) and bulk CsCl (Cl K-edge and Cs L_I edge). Data were collected and analysed over the same energy range as the s.e.X.a.f.s. data. Switching refined phase shifts from one compound to another gave agreement in the first-neighbour shell of better than 0.01 Å in each case. Provided, therefore, that the phase shifts from these bulk compounds can also be transferred to surface structures, the accuracy of our analyses would appear to be in the region of ± 0.01 Å.

It is concluded that s.e.X.a.f.s. has provided a structure determination for the adsorption of Cl on Ag{111} at coverages up to 0.7 monolayers. The adatoms are adsorbed into threefold hollow conventional substrate sites; repulsive interactions between adatoms result in spreading of the overlayer, with exclusion of nearest-neighbour sites at coverages up to 0.4 monolayers. The 0.7 monolayer $(\sqrt{3} \times \sqrt{3})$ R 30° structure is a vacancy-honeycomb (or graphitic) simple-overlayer structure. The Ag–Cl bond length is 2.70 ± 0.01 Å, independent of coverage between 0.4 and 0.7 monolayers, which is shorter than that (2.77 Å) in bulk AgCl.

6. Conclusions

The major advantages of s.e.X.a.f.s. as a structural tool are demonstrated by the accuracy and relative ease with which nearest-neighbour bond lengths have been determined for I on Ni{100} and for Cl on both Ag{100} and Ag{111}. For Ag{100}–$c(2 \times 2)$Cl, good agreement is obtained with the prior l.e.e.d. intensity analysis of Zanazzi *et al.* (1976), with some improvement in accuracy. The degree to which s.e.X.a.f.s. complements l.e.e.d. as a technique is, however, most clearly demonstrated with the analysis of both the weakly ordered Ag{111}–$(\sqrt{3} \times \sqrt{3})$ R 30°–Cl structure and the 0.4 monolayer disordered Ag{111}–Cl structure. Neither of these structures are amenable to a full l.e.e.d. intensity analysis. The usefulness of a full multishell analysis for structure determination at submonolayer coverages, sensitive to the fourth shell for the 0.7 monolayer Ag{111}–Cl structure and the third shell for the 0.4 monolayer structure, is illustrated for the first time with these studies.

The advantages in obtaining s.e.X.a.f.s. data at low temperatures are clearly demonstrated for the Ag/Cl system. For structures, such as this, where the mean square displacement of atoms is large, there are two advantages in cooling the crystal: an increase in the amplitude of the e.X.a.f.s. modulations as the scattering contribution from the Debye–Waller term is reduced, and the reduction of anharmonic terms that can give rise to incorrect bond lengths if ignored in the analysis. By using the demonstrated transferability of phase shifts between bulk compounds of known crystal structure, and making the reasonable assumption that these phase shifts are then transferable to comparable surface structures, it is concluded that first-shell bond length uncertainties of ± 0.01 Å have been achieved from low-temperature data. If the *correct* phase shifts are used on room-temperature data, however, errors of around 0.06 Å are introduced in bond lengths for the Ag/Cl systems. In practice this systematic error can be reduced by refining the phase shifts against bulk e.X.a.f.s. spectra from model compounds *at the same temperature* as the adsorbate-structure s.e.X.a.f.s. determination. The refined 'phase shift' then includes the anharmonicity term in (3), i.e. $\phi_i(k) + \Sigma_i(k)$. Provided the anharmonicity is

transferable from bulk compound to surface structure, the systematic error can be removed. However, since the mean square displacement of atoms at surfaces is generally larger than that for the equivalent bulk compound, it can be anticipated that a small systematic error is not eliminated by this *ad hoc* procedure. Lamble *et al.* (1985) have shown that for Cl on Ag{111}, transference of the refined 'phase shifts' from bulk AgCl at 300 K to the Ag{111}–($\sqrt{3} \times \sqrt{3}$) R 30°–Cl structure reproduces the nearest-neighbour spacing correctly, at 2.70 Å.

We acknowledge the S.E.R.C. for grants that enabled the development of the s.e.X.a.f.s. station at Daresbury jointly by groups from Liverpool University and Warwick University (D. O. Woodruff), and for a studentship to G.L. We are particularly grateful to all our colleagues who have participated in this work, including those based at Liverpool (R. Brooks, J. C. Campuzano, S. Ferrer) and at Daresbury (D. Norman, A. MacDowell), with special thanks to N. Binsted for assistance with computation.

References

Bowker, M. & Waugh, K. C. 1983 *Surf. Sci.* **134**, 639–664.
Citrin, P. H., Eisenberger, P. & Hewitt, R. C. 1978 *Phys. Rev. Lett.* **41**, 309–312.
Citrin, P. H., Eisenberger, P. & Hewitt, R. C. 1981 *Phys. Rev. Lett.* **45**, 1948–1951; erratum, *Phys. Rev. Lett.* **47**, 1567.
Citrin, P. H., Eisenberger, P. & Kincaid, B. M. 1976 *Phys. Rev. Lett.* **36**, 1346–1349.
Citrin, P. H., Hamman, D. R., Mattheis, L. F. & Rowe, J. E. 1982 *Phys. Rev. Lett.* **49**, 1712–1715.
Eisenberger, P. & Brown, G. S. 1979 *Solid State Commun.* **29**, 481–484.
Greenside, H. S. & Hamman, D. R. 1981 *Phys. Rev.* B **23**, 4879–4887.
Gurman, S. J., Binsted, N. & Ross, I. 1984 *J. Phys.* C **17**, 143–151.
Jaeger, R., Feldhaus, J., Haase, J., Stöhr, J., Hussain, Z., Menzel, D. & Norman, D. 1980 *Phys. Rev. Lett.* **45**, 1870–1873.
Jones, R. G., Ainsworth, S., Crapper, M. D., Somerton, C., Woodruff, D. P., Brooks, R. S., Campuzano, J. C., King, D. A., Lamble, G. M. & Prutton, M. 1985 *Surf. Sci.* **152/3**, 443–452.
Jones, R. G., McConville, C. F. & Woodruff, D. P. 1983 *Surf. Sci.* **127**, 424–440.
Lamble, G. M., Brooks, R., Campuzano, J. C., Ferrer, S., Norman, D. & King, D. A. 1985 (In preparation.)
Lee, P. A. 1976 *Phys. Rev.* B **13**, 5261–5270.
Lee, P. A. & Pendry, J. B. 1975 *Phys. Rev.* B **11**, 2795–2811.
MacDowell, A. A., Norman, D., West, J. B., Campuzano, J. C. & Jones, R. G. 1985 *Nucl. Instrum. Meth.* (In the press.)
Marsh, F. M. & King, D. A. 1979 *Surf. Sci.* **79**, 445–460.
Rovida, G. & Pratesi, F. 1975 *Surf. Sci.* **51**, 270–282.
Stern, E. A., Bunker, B. A. & Heald, S. M. 1980 *Phys. Rev.* B **21**, 5521–5539.
Stöhr, J., Denley, D. & Perfetti, P. 1978 *Phys. Rev.* B **18**, 4132–4139.
Weeks, S. P. & Rowe, J. E. 1978 *Solid St. Commun.* **27**, 885–889.
Zanazzi, E., Jona, F., Jepson, D. W. & Marcus, P. M. 1976 *Phys. Rev.* B **14**, 432–440.

Discussion

J. Wong (*Department of Physical Chemistry, Cambridge University, U.K.*). I would like to reinforce Professor King's comment that e.X.a.f.s. is still a young technique. With careful and detailed analysis, and under favourable conditions, bond distances can be determined to an accuracy of ± 0.02 Å. Furthermore, I would like to compliment Professor King's detailed and systematic analysis of the I on Ni(100) system presented here. In addition, I would like to draw attention to the part of the X-ray spectrum not discussed by Professor King. This is the so-called X.a.n.e.s. (X-ray absorption near-edge structure) spectrum, which arises from transitions from the core state (1s in K edge, $2p_{\frac{3}{2},\frac{1}{2}}$ in $L_{3,2}$ edges, 2s in L_1 edge, etc.) to some bound state in the upper valency region, and contains chemical information about the central X-ray absorbing atom

in terms of its valence, site symmetry, coordination geometry, ligand type as well as bond distances. Examples of these X.a.n.e.s. spectra can be seen in: (*a*) a series of vanadium oxides (VO, V_2O_3, V_4O_7, V_2O_4 and V_2O_5) reported recently (Wong *et al.* 1984); (*b*) Ti in octahedral and tetrahedral coordinations (Greegor *et al.* 1983); (*c*) *S* in various bonding configurations (Spiro *et al.* 1984) as well as (*d*) K in a variety of coordination geometries (Spiro *et al.* 1985). These studies show that the X-ray absorption spectrum contains both electronic (bonding) information as well as local atomic structure respectively in the X.a.n.e.s. and e.X.a.f.s. regions. With synchrotron radiation sources these spectra can now be measured routinely, more easily and with higher resolution than ever possible with X-ray tube sources.

References

Greegor *et al.* 1983 *J. non-cryst. Solids* **55**, 27.
Spiro *et al.* 1984 *Science, Wash.* **226**, 48.
Spiro *et al.* 1985 *Fuel.* (Submitted.)
Wong *et al.* 1984 *Phys. Rev.* B **30**, 5596.

D. Norman (*S.E.R.C., Daresbury Laboratory, Warrington, U.K.*). Following Dr Wong's comments about the value of the X.a.n.e.s. in determining oxidation state and solid state effects, I would like to point out that this region of the spectrum is also receiving attention in surface studies. For atomic adsorbates, the interpretation is complex, relying on multiple-scattering calculations, but the adsorption site of O on Ni(001) has been confirmed by such work (Norman *et al.* 1983); however, for molecular adsorbates, the X.a.n.e.s. is often dominated by transitions to π^* and σ^* intra-molecular resonances, and can be very simply understood (Norman & Durham 1983). Such spectra have yielded the details of orientation and bonding for several molecular species (Stöhr *et al.* 1983), and hold the prospect of shedding light on several of the problems mentioned by Professor Somorjai and Professor Yates in their papers at this symposium.

References

Norman, D., Stöhr, J., Jaeger, R., Durham, P. J. & Pendry, J. B. 1983 *Phys. Rev. Lett.* **51**, 2052.
Norman, D. & Durham, P. J. 1983 *SPIE Proc.* **447**, 102.
Stöhr, J., Gland, J. L., Eberhardt, W., Outka, D., Madix, R. J., Sette, F., Koestner, R. J. & Doebler, U. 1983 *Phys. Rev. Lett.* **51**, 2414.

PHILOSOPHICAL TRANSACTIONS OF THE ROYAL SOCIETY A MATHEMATICAL, PHYSICAL & ENGINEERING SCIENCES